Article citation info:
Szeszycki A, Bryk K, Stefańska N. Review and comparison of selected methods of calculating wheel-rail contact tangential forces on the example of riding stability analysis of a two-axle vehicle. Rail Vehicles/Pojazdy Szynowe. 2024;1-2:21-29. https://doi.org/10.53502/RAIL-186987

Rail Vehicles/Pojazdy Szynowe

www.railvehicles.eu

Review and comparison of selected methods of calculating wheel-rail contact tangential forces on the example of riding stability analysis of a two-axle vehicle

Adrian **Szeszycki** [a,b *], Karol **Bryk** [b], Natalia **Stefańska** [a,b]

[a] *Łukasiewicz Research Network – Poznań Institute of Technology, Center of Modern Mobility, Poland*
[b] *Poznan University of Technology, Faculty of Civil and Transport Engineering, Poland*

ARTICLE INFO

Received: 9 November 2023
Revised: 14 January 2024
Accepted: 9 April 2024
Available online: 27 April 2024

KEYWORDS

Railway vehicle dynamics
Multibody simulation
Wheel-rail contact
Kalker theories
FASTSIM
CONTACT

This article presents methods currently used in railway vehicle dynamics simulations (MBS) for calculating wheel-rail contact forces. Simulation models of two-axle vehicle built in Simpack 2023 simulation environment were used to compare the selected methods. The paper focuses on the issue of riding stability of the mentioned group of vehicles. The develoed research methodology consists in simulating the riding of a vehicle exhibiting instability (hunting movement) on an ideal straight track using the wheel-rail contact models available in the Simpack 2023 environment. Then the obtained results are input data for recalculation of contact forces with selected algorithms. The study is aimed at comparing the selected methods for calculating contact forces, so there is no interaction of the algorithms tested with the MBS simulation model. The results obtained were compared with Kalker's "exact theory" of contact (CONTACT) for the elliptical contact area.

1. Introduction

In the analysis of rail vehicle dynamics, it is important to find the response of the wheel-rail system to applied loads. The wheel-rail interaction is responsible for transferring vehicle mass, guiding forces, and excitations from track irregularities, so it is a priority issue for riding dynamics. Modeling the contact is most simply accomplished by point contact of rigid bodies on a plane or in space. In many fields this approach is sufficient, but when considering the dynamics of railway vehicles, it is necessary to take into account the deformation of the contacting bodies. This involves forming of a contact area of about 1.5 cm^2 in size for typical railway vehicles. Due to difficulties of experimental testing, usage of simulation studies to analyze the issue is common. Accurate and computationally efficient models are necessary for railway vehicle dynamics simulations. The present work includes a comparison of selected methods of calculating the tangential forces of wheel-rail contact, which have had the most significant influence on simulations of railway vehicle dynamics. The paper includes an evaluation of the simplified method of calculating tangential forces results in relation to the "exact" method under conditions accompanying the hunting oscillation of two-axle vehicle.

2. Contact mechanics and Kalker's rolling contact theories

2.1. Contact mechanics

In order to present the analyzed methods of calculating tangential contact forces, it is necessary to introduce the basic issues related to the determination of the state of deformation and stress in the areas of contact between two bodies, which is dealt by contact mechanics. Most of the consideration of the wheel-rail contact problem will be limited to the so-called elastic half-space approximation, in which local fragments of the contact bodies (wheel and rail) are replaced by elastic half-spaces. Such an approach will give considerable advantage due to the known exact stress-

* Corresponding author: adrian.szeszycki@pit.lukasiewicz.gov.pl (A. Szeszycki)

strain relationships for a given load however, it involves the following assumptions [3]:

– Linear elastic behavior of homogeneous isotropic material and assumption of linear (small) elastic strain
– Small contact area compared to the radii of curvature of the bodies near the contact
– Non-conforming bodies (a flat contact area).

Heinrich Hertz found a solution of the contact problem of elastic half-spaces. Hertz in his theory, relied on the hypothesis that the formed contact region in general assumes an elliptical shape, which was confirmed by elasto-optical observations. This approach is valid if in addition to the mere assumptions of the elastic half-spaces approximation, further assumptions are introduced:

– No tangential forces in contact
– Smooth contact surfaces that can be described by a quadratic function - constant radii of curvature.

In the Hertz description of contact solids, the undeformed surface distance function is the difference of the elliptic paraboloid functions that describe the principal radii of curvature of bodies 1 and 2: R_{1x}, R_{2x} in the y-z plane and R_{1y}, R_{2y} in the x-z plane. The radii are taken to be positive when the surfaces are convex. When the planes of the main curvature radii of the bodies are congruent, the undeformed distance function as a function of x and y coordinates is:

$$h = Ax^2 + By^2$$
$$A = \frac{1}{2}\left(\frac{1}{R_{1y}} + \frac{1}{R_{2y}}\right) \quad (1)$$
$$B = \frac{1}{2}\left(\frac{1}{R_{1x}} + \frac{1}{R_{2x}}\right)$$

Considering the situation before the load application, the solids contacts at a single point, which is taken as the origin of the coordinate system. The z axis of this system coincides with the direction normal to the contact surface. After the application of a normal load, the contact bodies, treated as rigid solids, penetrate each other to a maximum of a depth denoted by δ as shown on Fig. 1. According to the law of contact formation, the elastic deformation must compensate this distance.

The contact mechanics finds how the surface will deform under load relative to the undeformed state represented by the solid and dashed lines in Fig. 1, respectively. According to the Hertz's theory, deformed surfaces are in contact in an elliptical region. The eccentricity of this ellipse is not depended on the applied load but only on the radii of curvature of the contact solids. The distribution of normal contact stresses in the contact area of Hertz's theory takes the form:

$$p_n = p_0\sqrt{1 - \left(\frac{x}{a}\right)^2 - \left(\frac{y}{b}\right)^2} \quad (2)$$
$$P = \frac{2}{3}p_0\pi ab$$

where: p_0 – maximum pressure, P – normal force acting on contact bodies, a, b – half-axes of the contact ellipse in the x-axis and y-axis directions, respectively.

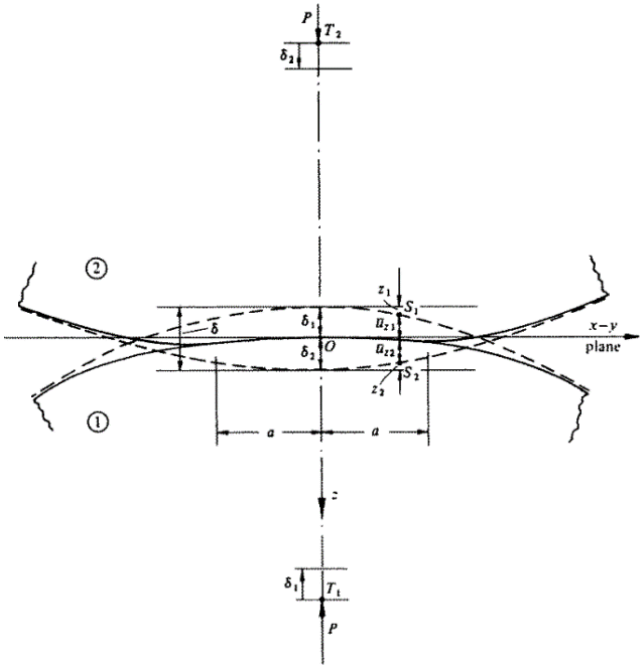

Fig. 1. Intersection of undeformed surfaces – dashed line, profile of deformed surfaces – solid line [3]

The analytical form of the Hertz contact solution allows for easy implementation in rail vehicle dynamics simulations due to its high computational efficiency. However, it involves a number of assumptions that, if not met, can lead to incorrect results. In addition, Hertz's description solves only the problem of normal contact, which, for the purpose of railway dynamics analyses, should be supplemented with a description of tangential behavior taking friction into account. Over the years, many complete theories of rolling contact have been developed, such as the theory of Carter and Fromm, Johnson, Johnson and Vermeulen [12]. For the purposes of this article, Kaler's theories will be presented, which form the basis of the methods currently used to calculate wheel-rail contact forces.

Consideration of rolling contact theories should begin with the definition of slip, which means the relative velocity of two material particles in contact as [6]:

$$s = c - \frac{\partial u}{\partial x}v + \frac{\partial u}{\partial t} \quad (3)$$

where: $c = \dot{x}_1 - \dot{x}_2$ – rigid slip resulting from the motion of bodies as rigid bodies, $u = u_1 - u_2$ – difference of elastic displacements, $x = \frac{1}{2}(x_1 + x_2)$ – middle coordinate, $v = -\dot{x}$ – rolling velocity.

Rigid slip, in addition to relative linear velocities, consists of angular velocity difference with respect to the normal axis, or so-called spin.

2.2. Kalker's linear theory

Kalker's linear theory applies to the case without slip, i.e., it applies when the rigid linear slip and spin have values close to zero or the coefficient of friction goes to infinity. This corresponds to the condition in which the friction limit is not exceeded and the entire contact area is covered by the adhesion region. In his dissertation, Kalker considered the case of an elliptical contact in which the direction of rolling is close to or coincident with one of the directions of the ellipse axis [5]. Starting from the definition of slip when its value equals 0, one can obtain relations for the elastic displacements difference in the two tangent directions [6].

$$u_x = \xi x - \phi xy + f(y) \tag{4}$$
$$u_y = \eta x + \frac{1}{2}\phi x^2 + g(y)$$

where: ξ – relative rigid slip (creepage) in the x-axis direction (rolling direction), η – relative rigid slip (creepage) in the y-axis direction, ϕ – relative spin, $f(y), g(y)$ – continuous y-functions as integration constants.

It is possible to approximate the functions f(y) and g(y) using polynomials of degree M. The choice of high degree polynomials led to accurate functions f(y) and g(y). Kalker, in his linear theory, found the functions f(y) and g(y) in such a way that the tangential stresses vanish at the leading edge of the contact. This results in a distribution of tangential stresses increasing in the contact area from zero starting at the leading edge and suddenly released at the trailing edge of the area [2].

Integrating the tangential stresses over the ellipse region leads to the determination of linear relationships: the total tangential forces F_x and F_y and the torque M_z as a function of the creepage.

$$F_x = -GabC_{11}\xi$$
$$F_y = -GabC_{22}\eta - G(ab)^{\frac{3}{2}}C_{23}\phi \tag{5}$$
$$M_z = -G(ab)^{\frac{3}{2}}C_{32}\eta - G(ab)^2C_{33}\phi$$

where: G – resultant Kirchhoff modulus of materials, C_{ij} – tabularized e.g. in [6] creepage coefficients, also called Kalker coefficients.

2.3. Kalker's simplified theory

In order to enable calculations for arbitrary creepage while maintaining high computational efficiency, Kalker developed a simplified theory to solve the tangential problem. Its main idea is to abandon exact constitutive relationships for elastic half-spaces replaced by a simple linear relationship between all contacting particles.

$$u_\tau = Lp_\tau \tag{6}$$

where: $\tau = x, y$ – directions of tangential axes, L – stiffness parameter.

The model for such material behavior is a perfectly rigid body covered with springs with tangential stiffness L [2]. The conceptual scheme of that model is shown on Fig. 2.

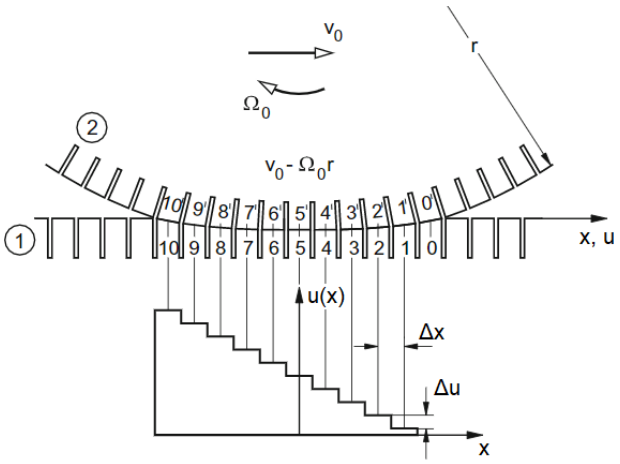

Fig. 2. Material model of contact solids of Kalker simplified theory, based on [7]

Due to the assumed constitutive relationship, the elastic displacement of each conceptual spring increases linearly, as shown in Fig. 2. The assumption of zero tangential stresses on the leading edge of an elliptical contact area leads to the following formulas for total tangential forces in the case of vanishing slip:

$$F_x = -\frac{8a^2b\xi}{3L} \tag{7}$$
$$F_y = -\frac{8a^2b\eta}{3L} - \frac{\pi a^3 b\phi}{4L}$$

By comparing the coefficients prior creepages in the formulas for the total tangential forces of the simplified theory and the linear theory without slips, it is possible to determine the values of the 3 stiffness coefficients associated with the corresponding creepage (and spin).

$$L_1 = \frac{8a}{3GC_{11}}$$

$$L_2 = \frac{8a}{3GC_{22}} \tag{8}$$

$$L_3 = \frac{\pi a^2}{4G\sqrt{ab}C_{23}}$$

Subsequently, Kalker in a simplified theory proposed a resignation from the distribution of normal stresses consistent with Hertz's theory. More accurate results of the total contact forces and the division of the contact area into zones of adhesion and slip are given by the parabolic distribution of the friction boundary g:

$$g = fp_n = f\frac{2P}{\pi ab}\left(1 - \left(\frac{x}{a}\right)^2 - \left(\frac{y}{b}\right)^2\right) \tag{9}$$

f – Coulomb coefficient of friction.

2.4. Kalker's "exact" theory

Kalker's "exact" theory uses a variational approach to the contact issue. The aforementioned theory has been called exact because it does not simplify material constitutive law, but note that it is still limited for cases satisfying assumptions for linear materials of elastic half-spaces. However, it is not necessary to meet the assumptions of Hertz's theory, since Kalker's method allows solutions also for a non-elliptic contact region. By deriving the "exact" theory, it is possible to begin with the principle of virtual work or complementary virtual work [2, 6]. In the case of the latter, the function whose maximization leads to the solution takes the form:

$$\max_{u,p} E = -\int_{A_c}\left(h + \frac{1}{2}u_n\right)p_n dA - \int_{A_c}\left(C_\tau + \frac{1}{2}u_\tau - u'_\tau\right)p_\tau dA \tag{10}$$

sub:

$$p_n \geq 0, |p_\tau| \leq g$$

where: $C_\tau = \int_{t'}^{t} c_\tau dt$ – rigid particle shift between time steps t' and t, u'_τ – difference of tangential elastic displacements from the previous time step.

The first integral of the maximized function corresponds to the normal problem, and the second to the tangent problem. Under all conditions, Kalker proved the existence and uniqueness of the solution in the global maximum E.

It will be useful for solving Kalker's "exact" theory to use the solutions of the Boussinesq and Cerutti problems. This concerns the determination of the state of stress, strain and displacement field of an elastic half-space quasi-statically loaded with a normal and tangential concentrated force, respectively [10]. This allows finding the influence function A connecting the stresses in the k-direction at the y-point with the displacements in the i-direction of the x-point belonging to the A_c contact area.

$$u_i(x) = \iint_{A_c} A_{ik}(x,y)p_k(y)dA \tag{11}$$

3. Methods for calculating tangential forces of wheel-rail contact

3.1. FASTSIM algorithm

In the absence of spin in relative rigid slips, it is possible to analytically determine the division into adhesion and slip zones and calculate contact forces using simplified Kalker theory. Otherwise, a numerical method is necessary. Therefore, an algorithm called FASTSIM was developed, in which the contact area is discretized [4].

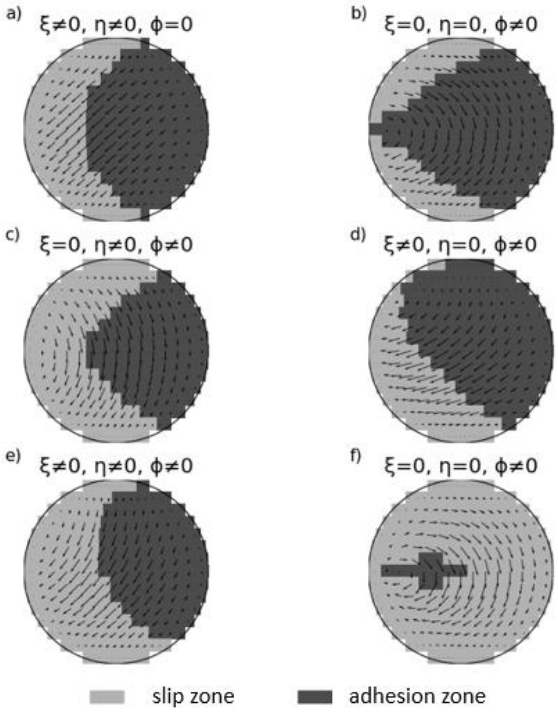

Fig. 3. Examples of dividing the contact area into adhesion and slip zones determined by the FASTSIM algorithm (case (b) – low spin, (f) – high spin)

The proposed discretization of the contact ellipse consisted of dividing the area into n strips consistent with the rolling direction and dividing each strip into m equal rectangular elements. The FASTSIM algorithm works in two loops: the outer one iterating over the discretization strips and the inner one over the elements in a given strip. The calculation of tangential contact stresses follows for each strip starting from the leading edge of the ellipse, where their value is 0. Then the stresses increase linearly according to the value of the stiffness parameter L, checking each time the Coulomb friction limit condition. If the limit as-

sumed for the simplified theory in a given element is exceeded it goes into the slip zone and the tangential stresses scale up to the friction limit. Figure 3 shows an example of the results of division the contact area, characteristic for different creepage cases.

Contrary to earlier approximate methods of solving the wheel-rail contact problem, the FASTSIM algorithm copes well with cases of significant spin. Finding the directions of tangential stresses in the presence of spin is not trivial and its effect is clearly visible in solutions using the FASTSIM algorithm (Fig. 3).

3.2. CONTACT program

The solution of the contact problem of the Kalker "exact" theory for the Hertzian cases and rigid slips close to zero is the presented solution of the linear Kalker theory. For the other cases, it is necessary to use a numerical method. For this reason, a program called CONTACT was developed in the 1980s, which allows the solution of both the normal and tangential problem in terms of the elastic half-space approximation. In CONTACT, the area of potential contact is discretized into rectangular elements whose principal axes coincide with the rolling direction – the x-axis and the direction perpendicular to it – the y-axis. The quantities sought are calculated at the geometric centers of each element, while assuming stepwise transition of contact stresses between elements. For the adopted discretization of the contact area, it is possible to determine the values of the stress-displacement influence function A between any elements by integration the Boussinesq and Cerutti solutions over the areas of these elements. Due to the assumption of equal material constants of the wheel and rail treated as elastic half-spaces, it is possible to solve the normal and then the tangential problem independently. In CONTACT, the iterative algorithms NORM and TANG, respectively, are responsible for this; for the purposes of the present study, it is sufficient to present only the solution of the tangential problem.

The TANG algorithm, based on the solution of the normal problem and the given creepage, determines the division of the contact area into zones of adhesion and slip and the tangential contact stresses. In each iteration of the determined division of the contact area, a system of linear equations in the adhesion zone and nonlinear equations in the slip zone is solved. If the calculated tangential stresses exceed the friction limit in some elements – they go to the slip zone and another iteration is performed, otherwise another condition about ensuring the opposite sense of the slip vector to the stress vector is checked. If there are elements that do not meet this condition – they go to the adhesion zone and another iteration is performed. If the conditions are met in all elements, the solution of the tangent problem is achieved [6]. Since the nonlinear equations occurring in the slip zone for a large number of discretization elements are computationally demanding, more efficient computational methods than the TANG algorithm for exact Kalker theory are pleased. The use of the Gauss-Seidel method to solve the aforementioned system of equations allowed the development of the more efficient ConvexGS [13] and SteadyGS [14] algorithms, which were used for the purposes of current research.

A comparison of the different traction bounds between the FASTSIM algorithm and the CONTACT program is shown in Fig. 4.

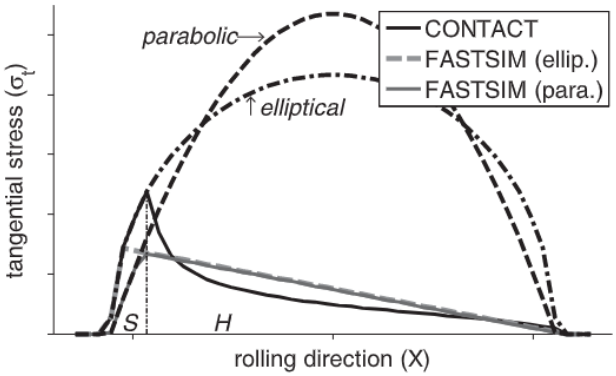

Fig. 4. Comparison of the elliptical (Hertz) tangential stress limit with the parabolic one adopted by Kalker in the simplified theory [8]

The above figure explains the reason why the FASTSIM algorithm for an elliptical tangential stress boundary gives more accurate results than using the Hertzian normal stress distribution. Namely, then, for the linear stress increment of the simplified theory, the division into adhesion and slip zones is obtained more closely to the exact theory.

3.3. Simpack 2023 methods

In the Simpack 2023 program used for the simulation studies carried out, two most important simplified methods for calculating wheel-rail contact forces are available, called equivalent-elastic and discrete-elastic. The two methods, in order to determine the shape of the contact area, are based on the virtual interpenetration of the contact solids as rigid bodies, but in a different way.

The equivalent-elastic method converts the area of virtual penetration into an ellipse, whose axes have dimensions corresponding to the maximum length and width of the interpenetration area. The virtual penetration value corresponding to the ellipse is determined for a piece of a circle with a width and an area equal to the y-z cross-sectional area of the virtual penetration solid [16]. Since the actual penetration corre-

sponding to the equivalent ellipse is larger, for the purpose of further calculations the penetration value is scaled by a factor of 0.55 taken from [9]. For the ellipse half-axes and equivalent penetration determined in this way, the tangential contact stresses are determined using the FASTSIM algorithm [16].

The discrete-elastic method is more advanced, allowing calculations for non-elliptical contact areas, and is based on the method of Ayasse and Chollet [1, 11]. The solution to the normal problem is so-called semi-Hertzian because it takes advantage of the fact that the radii of curvature remain constant in the rolling direction giving a Hertzian distribution of normal contact stresses in that direction. Ayasse and Chollet, in their simplified method, aimed to maintain the results coinciding with the Hertz method when an elliptical contact area was present. Since the shape of the ellipse of the virtual geometric interpenetration area does not correspond exactly to the shape of the actual contact ellipse except in the circular area, a correction of curvatures A and/or B based on the Hertz solution is introduced. In addition, when the change of curvature B is stepped which is the case for standard wheel and rail profiles, the resulting virtual penetration contact area has sharp variation, which does not occur in reality. This problem was solved by introducing a smoothing function of the boundary of the contact area [1, 11]. In the method under discussion, the determined contact area is discretized analogously to the original FASTSIM method. The solution of both the normal problem by the Hertz method and the tangent problem by the FASTSIM algorithm is carried out independently for each discretization strip, taking into account local parameters such as:

– strip length
– the actual principal radii of curvature of the wheel and rail
– the slope of the wheel and rail profiles
– the value of maximum penetration
– creepage values.

4. Methodology of comparative study on algorithms for calculating wheel-rail contact tangential forces

A numerical model of the WM-15C two-axle vehicle was created in Simpack 2023 software. The vehicle under study is a typical track maintenance machine with link suspension and fork guidance of the wheelsets. Depreciation is provided by coil springs and leaf springs which were modeled taking into account the deflection hysteresis loop determined by FEM simulation. Friction occurring in the link suspension was also modeled using advanced friction elements. The wheel-rail contact model was the equivalent-elastic method. A view of the graphical representation of the numerical model is shown in Fig. 5.

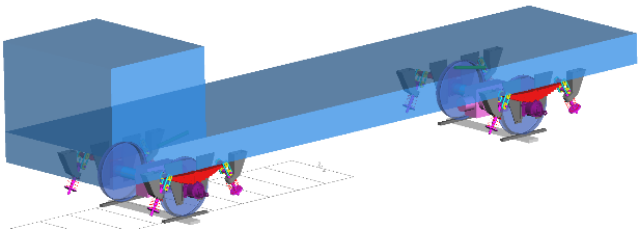

Fig. 5. View of the WM-15C vehicle model in Simpack 2023

The mass elements were modeled as perfectly rigid bodies with the topology shown in the figure above.

Unstable riding of two-axle vehicles often occurs in normal operation even below the maximum allowable speed. This is an unfavorable phenomenon, so it is important to confirm the validity of the results obtained by typical calculation methods. Running instability is associated with hunting motion of wheelsets, the simplest description of which is the kinematic sinusoidal motion of a wheelset with tapered wheels on line rails. The wavelength of that motion is described by the Klingel formula [17]:

$$\Lambda = 2\pi\sqrt{\frac{r_0 l}{\lambda}} \tag{12}$$

where: r_0 – radius of the wheel, l – half of the rail spacing, λ – conicity of the wheel profile defined by the tangent of half the angle of the cone.

For real wheelsets in the track, the concept of equivalent conicity applies, which at a certain amplitude gives the same wavelength of the real wheelset as the pure conic one. A railway vehicle is called stable - if the hunting motion of the wheelsets tends to disappear. The maximum speed at which the vehicle is still stable is called the critical speed of the vehicle.

For the purposes of the study, it was decided to test stability on an ideal straight track at a speed of 90 km/h (maximum allowable speed +10 km/h), introducing an initial wheelsets lateral displacement of 3 mm. The tests were carried out for different values of equivalent conicity. The equivalent conicity value of 0.18 corresponded to a nominal standard wheel profile S1002 on S60 rail with an inclination of 1:40, a value of 0.4 to a worn wheel profile S1002 on the same rail and a value of 0.05 to a nominal standard wheel profile of S1002 on S49 rail with an inclination of 1:20. The trajectories of the lateral displacement of the wheelsets obtained for the tested conicities are shown in Fig. 6–8.

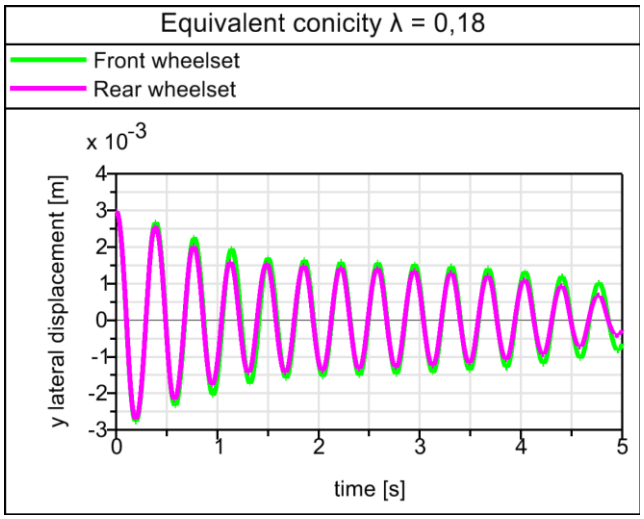

Fig. 6. Wheelset lateral displacement for equivalent conicity of 0.18

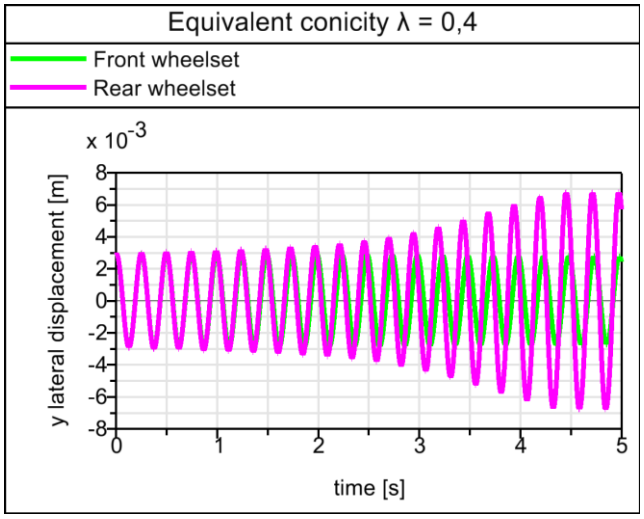

Fig. 7. Wheelset lateral displacement for equivalent conicity of 0.4

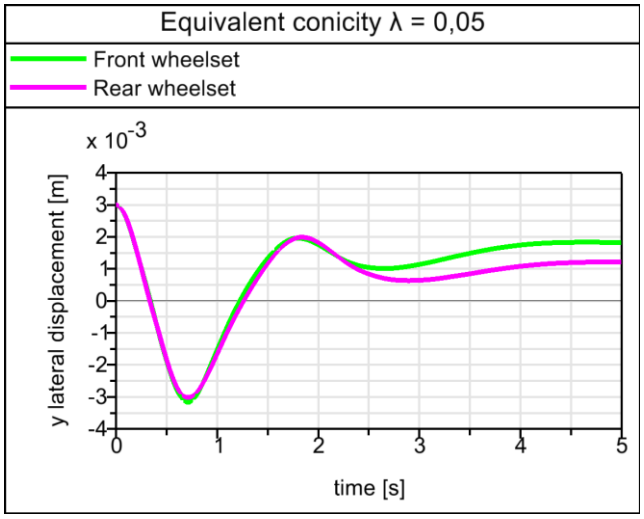

Fig. 8. Wheelset lateral displacement for equivalent conicity of 0.05

For tested equivalent conicities different behaviors are visible: for high conicity the vehicle is clearly unstable – the amplitude of oscillations increases rapidly (Fig. 7) on the other hand for low conicity after one cycle the oscillations decay (Fig. 8). A comparison of algorithms for calculating tangential contact forces was made for a single cycle of the hunting motion (some of the first cycles from Fig. 6–8). The selected simulation time instances using the method for calculating tangential contact forces implemented in Simpack 2023 provided the wheel-rail contact conditions accompanying the stability study of 2-axle vehicle. The resulting values of creepage, shape of the contact area and normal contact stresses provided input for calculations using the CONTACT method of tangential problem solving.

5. Results

The results of the total tangential forces and the corresponding distributions of tangential stresses and the division of the contact area into adhesion and slip zones were obtained. Figures 9–11 show the tangential force curves of the right rear wheel for one cycle of hunting movement for different values of equivalent conicity.

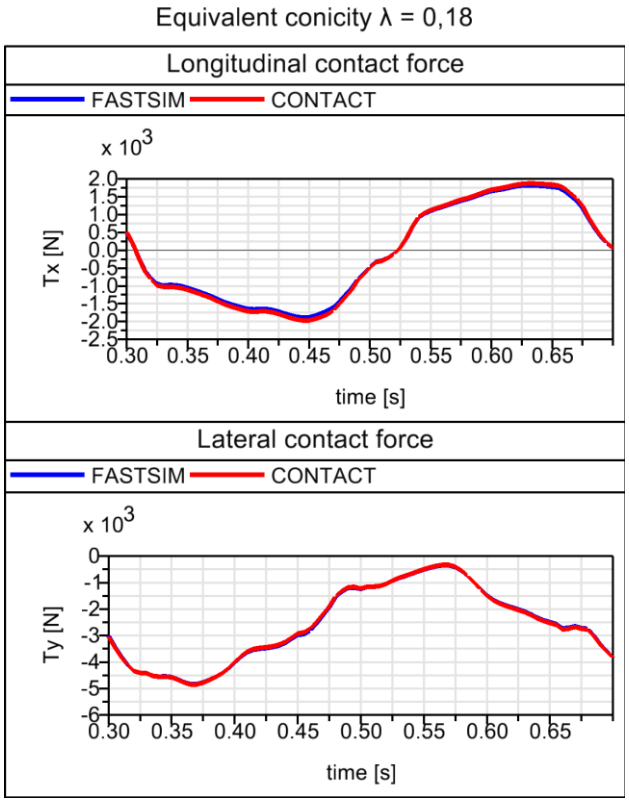

Fig. 9. Tangential contact forces of the right wheel of the rear wheelset for an equivalent conicity of 0.18

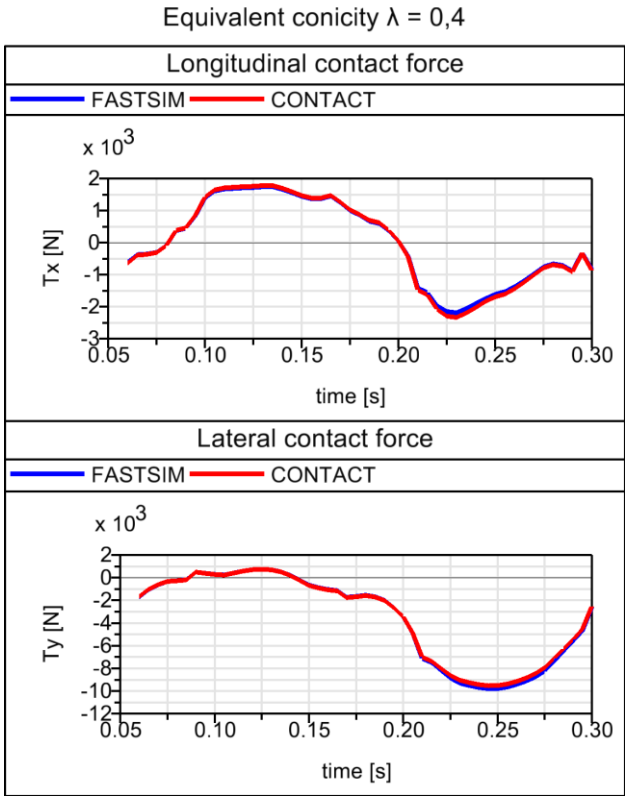

Fig. 10. Tangential contact forces of the right wheel of the rear wheelset for an equivalent conicity of 0.4

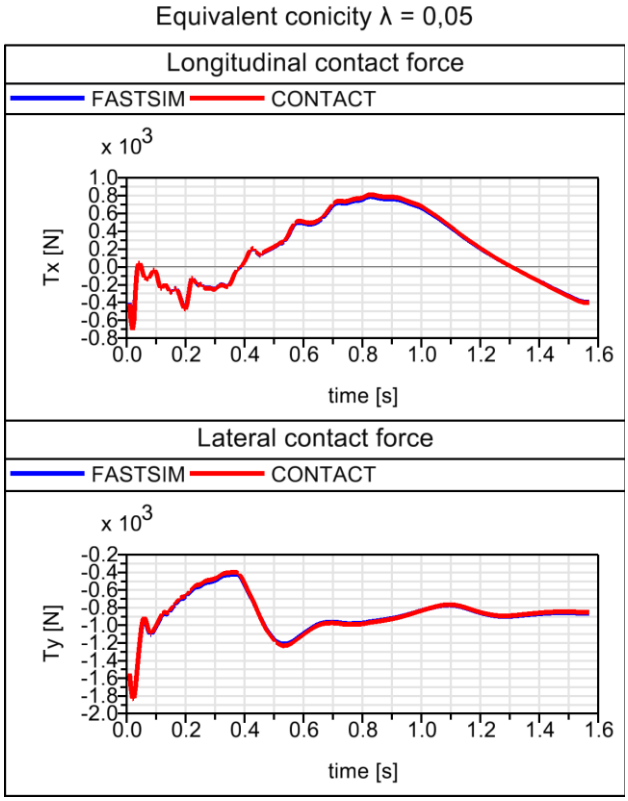

Fig. 11. Tangential contact forces of the right wheel of the rear wheelset for an equivalent conicity of 0.05

The largest values of tangential contact forces were reached for an equivalent conicity of 0.4 and the smallest for 0.05 what is visible in Fig. 9–11. In addition, the lateral force reaches greater values than the longitudinal force in all cases. The resulting tangential stress distribution of the case corresponding to the maximum value of the lateral force is presented in Fig. 12.

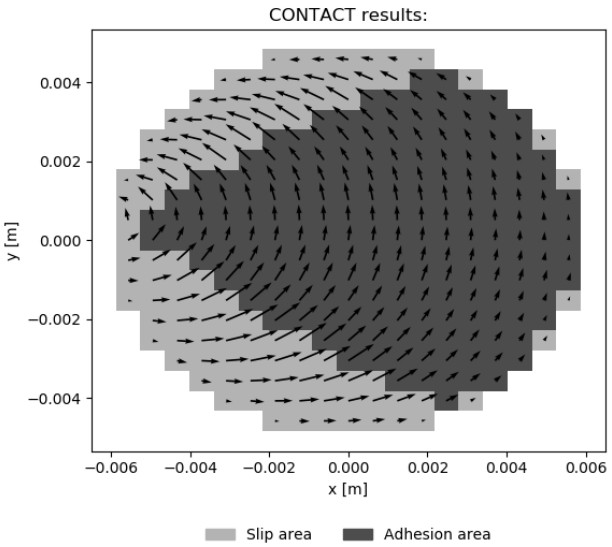

Fig. 12. Distribution of tangential contact stresses and division of the contact area into zones of adhesion and slip of the right rear wheel for a time instant of 0.25 s in the case of an equivalent conicity of 0.4

6. Summary

The total tangential forces have a direct influence on the dynamic behaviour of the vehicle, in particular the riding stability, and these results are therefore the most relevant for the research conducted. As expected, the results of the total tangential forces for the elliptical contact areas converge for the two tested methods: FASTSIM and CONTACT. The largest differences in forces occur for an equivalent conicity of 0.4, for which the largest spin values occurred around the 0.25 s time instant. For such cases, the largest errors of the FASTSIM method were also found by other researchers [15]. This was associated with the formation of the largest share of the slip zone in the contact area (Fig. 12), for which the parabolic tangential stress limit adopted in the FASTSIM algorithm causes differences compared to the CONTACT method consistent with the Hertz solution. In addition, the difference in results may be slightly influenced by the different discretisation strategy of the contact area of the two methods.

The results of the stability tests themselves, in the form of the lateral wheelsets displacement curves, testify to the key role of equivalent conicity, for which

completely different values of contact lateral forces were obtained. Further comparative studies are therefore necessary to confirm the validity of the results of the simplified methods also for non-elliptical contact areas, as they should give more accurate results with respect to the methods restricted for the elliptical contact area due to the lack of fulfilment of the Hertz assumptions of wheel-rail contact.

Acknowledgements

The research was carried out under the Applied Doctorate Program of the Ministry of Education and Science implemented in the years 2021-2025 (agreement no. DWD/5/0358/2021 of 23.12.2021).

Nomenclature

CONTACT	numerical program of solving Kalker "exact theory" contact problem
F	forces
FASTSIM	numerical algorithms based on the simplified theory of Kalker
FEM	finite element method
M	torque
MBS	multibody simulation
NORM	numerical algorithm of solving Kalker "exact" theory contact problem in its normal part
TANG	numerical algorithm of solving Kalker "exact" theory contact problem in its tangential part

Bibliography

[1] Ayasse JB, Chollet H, Determination of the wheel rail contact patch in semi-Hertzian conditions. Vehicle Syst Dyn. 2005;43(3):161-172. https://doi.org/10.1080/00423110412331327193

[2] Jacobson B, Kalker JJ. Rolling contact phenomena: linear elasticity. Springer Vienna 2000. https://doi.org/10.1007/978-3-7091-2782-7

[3] Johnson KL. Contact mechanics. Cambridge University Press, 1985. https://doi.org/10.1017/CBO9781139171731

[4] Kalker JJ. A fast algorithm for the simplified theory of rolling contact. Vehicle Syst Dyn. 1982; 11(1):1-13. https://doi.org/10.1080/00423118208968684

[5] Kalker JJ. On the rolling contact of two elastic bodies in the presence of dry friction. Delft 1967. https://repository.tudelft.nl/islandora/object/uuid:aa44829b-c75c-4abd-9a03-fec17e121132/datastream/OBJ/download

[6] Kalker JJ. Three-dimensional elastic bodies in rolling contact. 1st ed., Springer Dordrecht 1990. https://doi.org/10.1007/978-94-015-7889-9

[7] Knothe K, Stichel S. Rail vehicle dynamics. Springer Cham 2016. https://doi.org/10.1007/978-3-319-45376-7

[8] Meymand SZ, Keylin A, Ahmadian M. A survey of wheel-rail contact models for rail vehicles. Vehicle Syst Dyn. 2016;54(3):386-428. https://doi.org/10.1080/00423114.2015.1137956

[9] Piotrowski J, Kik W. A simplified model of wheel/rail contact mechanics for non-Hertzian problems and its application in rail vehicle dynamic simulations. Vehicle Syst Dyn. 2008;46(1-2):27-48. https://doi.org/10.1080/00423110701586444

[10] Szeptyński P. Szczegółowe omówienie podstawowych zagadnień teorii sprężystości (in Polish). Wydawnictwo PK. Krakow 2020.

[11] Quost X, Sebes M, Eddhahak A, Ayasse JB, Chollet H, Gautier PE et al. Assessment of a semi-Hertzian method for determination of wheel-rail contact patch. Vehicle Syst Dyn. 2006;44(10):789-814. https://doi.org/10.1080/00423110600677948

[12] Vermeulen PJ, Johnson KL. Contact of nonspherical elastic bodies transmitting tangential forces. J Appl Mech. 1964;31(2):338-340. https://doi.org/10.1115/1.3629610

[13] Vollebregt EAH. A Gauss-Seidel type solver for special convex programs, with application to frictional contact mechanics. Optim Theory Appl. 1995; 87(1):47-67. https://doi.org/10.1007/BF02192041

[14] Vollebregt EAH. Improving the speed and accuracy of the frictional rolling contact model 'CONTACT'. The Tenth International Conference on Computational Structures Technology, 2010. https://doi.org/10.4203/ccp.93.17

[15] Vollebregt EAH, Iwnicki SD, Xie G, Shackleton P. Assessing the accuracy of different simplified frictional rolling contact algorithms. Vehicle Syst Dyn. 2012;50(1):1-17. https://doi.org/10.1080/00423114.2011.552618

[16] Vollebregt EAH, Weidemann C, Kienberger A. Use of "CONTACT" in multi-body vehicle dynamics and profile wear simulation: initial results. Proceedings of the 22nd International Symposium on Dynamics of Vehicles on Roads and Tracks. Manchester 2011. https://api.semanticscholar.org/CorpusID:110002388

[17] Wickens A. Fundamentals of rail vehicle dynamics. CRC Press. London 2003. https://doi.org/10.1201/9780203970997